Main Text Word Count: 3,950

Translational Evidence for Dopaminergic Alteration of Basal Ganglia Functional Connectivity in Persons with Schizophrenia

*Philip N. Tubiolo, MS[1,2,3], *John C. Williams, PhD[1,2,4], Roberto B. Gil, MD[2,5,6], Clifford Cassidy, PhD[2], Natalka K. Haubold, BA[2], Yash Patel, MS[2], Sameera K. Abeykoon, PhD[2], Zu Jie Zheng, BS[2,7], Dathy T. Pham[2,8], Najate Ojeil, PhD, MPH[5,6], Kelly Bobchin, BA[2], Eilon B. Silver-Frankel, BS[2], Greg Perlman, PhD[2], Jodi J. Weinstein, MD[2,5,6], Christoph Kellendonk, PhD[5,6,9], Guillermo Horga, MD, PhD[5,6], Mark Slifstein, PhD[2,5,6], Anissa Abi-Dargham, MD[1,2,5,6,10] & Jared X. Van Snellenberg, PhD[1,2,5,6,11]

*These authors contributed equally to this work

[1]Department of Biomedical Engineering, Stony Brook University, Stony Brook, NY 11794;
[2]Department of Psychiatry and Behavioral Health, Renaissance School of Medicine at Stony Brook University, Stony Brook, NY 11794;
[3]Scholars in BioMedical Sciences Training Program, Renaissance School of Medicine at Stony Brook University, Stony Brook, NY 11794;
[4]Medical Scientist Training Program, Renaissance School of Medicine at Stony Brook University, Stony Brook, NY 11794;
[5]Department of Psychiatry, Columbia University Vagelos College of Physicians and Surgeons, New York-Presbyterian / Columbia University Irving Medical Center, New York, NY 10032;
[6]New York State Psychiatric Institute, New York, NY 10032;
[7]College of Medicine, State University of New York Downstate Health Sciences University, Brooklyn, NY 11203;
[8]Department of Neurobiology and Behavior, Cornell University, Ithaca, NY 14853;
[9]Department of Molecular Pharmacology & Therapeutics, Vagelos College of Physicians and Surgeons, New York-Presbyterian / Columbia University Irving Medical Center, New York, NY 10032;
[10]Department of Radiology, Renaissance School of Medicine at Stony Brook University, Stony Brook, NY 11794;
[11]Department of Psychology, Stony Brook University, Stony Brook, NY 11794.

CORRESPONDING AUTHOR:
Jared X. Van Snellenberg
101 Nicolls Rd
Health Sciences Center 10-087J
Stony Brook, NY 11794
Tel: 631-638-0064
Jared.VanSnellenberg@stonybrookmedicine.edu

Short/Running Title: Basal Ganglia Alterations in Schizophrenia

Abstract

In prior work, a transgenic mouse model of striatal dopamine dysfunction observed in persons with schizophrenia (PSZ) exhibited dopamine-related neuroplasticity in the basal ganglia, a phenotype that has never been demonstrated in human PSZ. Consequently, we sought to identify a dopamine-related alteration of basal ganglia connectivity via working memory task-based and resting-state functional magnetic resonance imaging (fMRI), neuromelanin-sensitive MRI (NM-MRI), and positron emission tomography (PET), in unmedicated PSZ. In this case-control study, 37 unmedicated PSZ and 30 demographically matched healthy controls (HC) underwent resting-state fMRI; a subset of 29 PSZ and 29 HC also underwent working memory task-based fMRI. Additionally, 22 PSZ and 20 HC underwent NM-MRI and a preliminary subset of 7 PSZ and 4 HC underwent [^{11}C]-(+)-PHNO PET with amphetamine challenge. Outcome measures included: 1) task-state and resting-state functional connectivity (FC) between dorsal caudate (DCa) and globus pallidus externus (GPe), 2) NM-MRI contrast-to-noise ratio in substantia nigra/ventral tegmental area voxels associated with psychotic symptom severity, and 3) baseline and amphetamine-induced change in [^{11}C]-(+)-PHNO binding potential in DCa. PSZ displayed elevated DCa-GPe task-state FC, which was associated with increased NM-MRI contrast-to-noise ratio in the substantia nigra, decreased baseline DCa D2 receptor availability, greater amphetamine-induced DCa dopamine release, and worse working memory task performance. This in-vivo evidence of a dopamine-associated neural abnormality of DCa and GPe connectivity in unmedicated PSZ suggests a potential neurodevelopmental mechanism of working memory deficits in schizophrenia, which could be a critical step towards developing treatments for cognitive deficits.

Abbreviations

ANTs, Advanced Normalization Tools;

BGTC, basal ganglia-thalamo-cortical;

BOLD, blood-oxygen-level-dependent;

BP_{ND}, binding potential (non-displaceable);

CIFTI, connectivity informatics technology initiative;

CNR, contrast-to-noise ratio;

D1R, dopamine D1 receptor;

D2R, dopamine D2 receptor;

D2R-OE, dopamine D2 receptor overexpressing;

DCa, dorsal caudate;

DLPFC, dorsolateral prefrontal cortex;

DOPA, dihydroxyphenylalanine;

FC, functional connectivity;

FDR, false discovery rate;

fMRI, functional magnetic resonance imaging;

GABA, gamma-aminobutyric acid;

GEV-DV, generalized extreme value DVARS;

GPe, globus pallidus externus;

GPi, globus pallidus internus;

HC, healthy control;

HRF, hemodynamic response function;

IBZM, iodobenzamide;

IQR, interquartile range;

K_{ir}, inwardly rectifying potassium;

MNI, Montreal Neurologic Institute;

MP, motion parameter;

MSN, Medium spiny neuron;

NM-MRI, neuromelanin-sensitive magnetic resonance imaging;

NYSPI, New York State Psychiatric Institute;

PANSS, positive and negative syndrome scale;

PET, positron emission tomography;

PHNO, 4-propyl-9-hydroxynaphthoxazine;

PSZ, persons with schizophrenia;

ROI, region of interest;

RS, resting-state;

rs-FC, resting-state functional connectivity;

SD, standard deviation;

SE, standard error;

SN, substantia nigra;

SOT, self-ordered working memory task;

SPM12, Statistical Parametric Mapping 12;

STN, subthalamic nucleus;

ts-FC, task-state functional connectivity;

TE, echo time;

TR, repetition time;

VTA, ventral tegmental area;

WM, working memory

1. Introduction

Evidence of striatal dopamine dysfunction in persons with schizophrenia (PSZ) is among the most robust and consistently replicated findings in the neurobiology of schizophrenia. Studies with [^{18}F]DOPA show elevated presynaptic striatal dopamine synthesis in medication-naïve and medication-free PSZ [1,2], as well as individuals at clinical high risk for schizophrenia [3,4]. Studies using radiolabeled dopamine D2 receptor (D2R) antagonists [^{123}I]IBZM or [^{11}C]raclopride show increased amphetamine-induced tracer displacement in striatum in PSZ [5,6], while depletion of dopamine with alpha-methyl-para-tyrosine results in increased tracer binding in PSZ [7,8]. This suggests PSZ exhibit higher occupancy of D2Rs due to higher synaptic levels of DA, consistent with increased presynaptic dopamine release.

These findings spurred the development of a transgenic mouse model to mimic this abnormality and study the neurophysiological consequences of excess striatal D2R stimulation. D2R overexpressing (D2R-OE) mice have selectively increased expression of D2Rs in the caudate-putamen, temporally controllable via doxycycline [9]. D2R-OE mice display performance deficits in a working memory (WM) task that persist even if D2R overexpression is halted in adulthood [9], suggesting a neurodevelopmental cognitive deficit reminiscent of those seen in human PSZ [10,11].

D2R-OE mice also display striking neuroplasticity within the basal ganglia-thalamo-cortical (BGTC) circuit [12], which plays critical modulatory roles in motor, limbic, and cognitive functioning [13,14]. This circuit is comprised of two functionally opposed pathways, the “direct” and “indirect” pathways (**Figure 1**). While these pathways were initially thought to be anatomically segregated, tracing studies in rats and monkeys demonstrate that some direct pathway D1R-expressing medium spiny neurons (MSNs), which project to the globus pallidus internus (GPi; entopeduncular nucleus in rodents) and substantia nigra (SN) pars reticulata, bifurcate and send additional collaterals to the globus pallidus externus [GPe; 15,16]; these are termed “bridging collaterals,” as they bridge the direct and indirect pathways [12].

D2R-OE mice exhibit increased density of these bridging collaterals, which decreased when overexpression was halted in adult animals, but returned to elevated levels when D2R overexpression was restored. Haloperidol, a D2R antagonist, also reduces bridging collateral density in D2R-OE and wildtype animals, while D2R knockdown mice exhibit dose-dependent reductions in bridging collateral density [12], demonstrating a causal relationship between striatal D2R stimulation and bridging collateral density. Notably, bridging collateral density in D2R-OE mice was greatest in associative striatum (medial caudate-putamen), which receives input from associative cortical regions such as the dorsolateral prefrontal cortex (DLPFC) [12]. Concordantly, human studies of PSZ using higher-resolution PET imaging have shown greater baseline occupancy of D2Rs in associative striatum, especially in the dorsal caudate (DCa) [7,17].

Here, we sought to translate findings of increased bridging collateral density to human PSZ, hypothesizing that if this compensatory response to D2R overstimulation occurs in PSZ, it should be detectable as altered functional connectivity (FC) between the striatum (specifically DCa) and the GPe. However, evidence also suggests that: 1) any alteration in FC may only be observable in unmedicated PSZ, as D2R antagonists reduce bridging collateral density in rodents; 2) while altered anatomical connectivity should alter DCa-GPe FC, the expected direction of change is unclear—although striatal MSNs are GABA-ergic and thus inhibitory, net inhibition of a region is still metabolically demanding and can increase functional Magnetic Resonance Imaging (fMRI) Blood Oxygen Level-Dependent (BOLD) signal [18]; and 3) because striatal MSNs are hyperpolarized at rest, with low baseline firing rates and periodic bursting [19,20], it is possible that altered FC may only be apparent under conditions in which the affected basal ganglia circuitry is actively processing information and MSNs are activated by cortical (and nigral) inputs.

Consequently, we conducted a resting-state and WM task-state FC MRI study [see, e.g., 21-31] of unmedicated PSZ, using a WM task that robustly activates the DCa and other striatal

regions [32]. We aimed to detect altered DCa-GPe connectivity, observable either during WM task engagement only or during both task engagement and at rest, consistent with increased bridging collateral density in PSZ as predicted by studies of D2R-OE mice.

Given the interconnected nature of the BGTC circuit, we chose to implement a network modeling approach to calculating FC between regions [see, e.g., 33]. This addresses the “third variable” problem, in which altered FC between regions could be driven by a third region that is not accounted for in the model (e.g., altered striato-pallidal connectivity could be driven by altered pallido-thalamic or cortico-striatal connectivity). Our approach calculates FC as partial correlations, controlling for timeseries in regions of interest (ROIs) outside each given ROI pair, a straightforward method that reliably distinguishes between direct and indirect network connections in simulated and *in vivo* data [33,34]. Additionally, this approach partially accounts for partial volume effects arising in adjacent network structures (e.g., pallidal subdivisions) that could otherwise inflate FC estimates.

Many of our participants were also enrolled in other neuroimaging studies, which included studies of dopamine function that could further inform whether altered FC might be driven by striatal dopamine dysfunction. Thus, in two subsets of our sample, we also report on the relationship between DCa-GPe FC and dopamine function measured via 1) neuromelanin-sensitive MRI (NM-MRI) of the SN [an indirect measure of long-term dopamine turnover that is correlated with psychotic symptoms; 35,36] and; 2) Positron Emission Tomography (PET) with the D2/3 agonist radiotracer [^{11}C]-(+)-PHNO [37,38] and an amphetamine challenge; however, the number of available PET participants was small (n = 11 across both groups), and thus should be taken as preliminary evidence that may support further investigation with appropriately powered samples. Finally, we conducted exploratory analyses examining the relationship between DCa-GPe connectivity and WM task performance and positive and negative symptoms in PSZ.

2. Materials and Methods

2.1. Overview

This is a case-control study of unmedicated PSZ and healthy controls (HC) aged 18-55 years old and demographically matched on age, parental socioeconomic status, race, and ethnicity. All procedures occurred at the New York State Psychiatric Institute (NYSPI) except PET scanning, which occurred at Yale University. PSZ were considered unmedicated if they were antipsychotic-naïve or antipsychotic-free for at least three weeks prior to recruitment. Additionally, antipsychotic-naïve participants had no prior use of long-acting injectable antipsychotics and less than 2 weeks of cumulative lifetime antipsychotic exposure. All participants were free of major neurological disorders, current substance use disorders, and psychiatric disorders other than schizophrenia, schizophreniform disorder, or schizoaffective disorder. Full inclusion and exclusion criteria are described in the **Supplementary Methods.** All procedures were approved by the NYSPI and Yale Institutional Review Boards. This study's overall hypothesis, including the focus on the specific associative striatum/GPe subcircuit discussed here and use of task-state and resting-state FC and the network modeling analytic approach employed, were defined prior to enrollment and stated explicitly in the original NIH RePORTER abstract of the award that funded this work [1K01MH107763; see 39] alongside a separate, independent hypothesis reported elsewhere [40], but was not formally pre-registered.

2.2. Participants

Thirty-seven PSZ and 30 HC completed RS fMRI, with a subset of 29 PSZ and 29 HC completing task-based fMRI. Additionally, 22 PSZ and 20 HC who performed task-based fMRI underwent NM-MRI. Finally, a smaller subset of task-based fMRI participants, 7 PSZ and 4 HC, underwent [^{11}C]-(+)-PHNO PET with amphetamine challenge as part of a separate and unrelated study (currently unpublished). Participants completed several clinical and demographic assessments described in the **Supplementary Methods** and reported in **Table 1**. RS fMRI data and NM-MRI data from a subset of these participants has been reported

elsewhere [35,40], while task-based fMRI data were acquired specifically for testing the *a priori* hypothesis presented in this manuscript, due to the concern that hyperpolarized striatal MSNs may not exhibit altered FC when not receiving substantial excitatory input from cortex.

2.3. Neuroimaging Procedures

MRI equipment, sequences, and processing are described in the **Supplementary Methods.** Briefly, in addition to standard structural sequences, we collected multiband fMRI scans with 2 mm isotropic voxel resolution for approximately 30 minutes each for RS and task-state FC (ts-FC). We employed the self-ordered WM task [SOT; see Figure S1 for task schematic; 32,41]; neural responses to task-events were modeled as per our prior work [32,42]. WM task fMRI data were then residualized with respect to modeled task-evoked activation to distinguish ts-FC from task-related coactivation [43,44]. Preprocessing was conducted with the Human Connectome Project Minimal Preprocessing Pipeline [45], version 4.2.0, followed by established FC-specific processing methods from prior work [46]. Finally, ts-FC used only "task-on" volumes, which were identified as volumes beginning two seconds after each task block onset and ending four seconds after the final trial of the block to account for the initial delay in hemodynamic response and gradual return to baseline [47].

To use network modeling to estimate FC, we identified a set of regions in the BGTC circuit with established roles in cognitive and associative functions: the mediodorsal nucleus (MD), DCa, GPe, GPi, SN, and DLPFC (see **Supplementary Methods** for identification procedures, **Figures S2**, **S3** for ROI visualizations). We omitted the subthalamic nucleus from this model, despite its importance in the indirect pathway, due to its small size and the lack of a reliable localization technique. Note that subcortical ROI timeseries were extracted using participant-specific ROI definitions.

NM-MRI was acquired and processed as described elsewhere [35; and see Supplementary Methods]. Our NM-MRI outcome measure was the average contrast-to-noise ratio (CNR) extracted from *a priori* voxels within an overinclusive mask of the SN and ventral tegmental area

(VTA), used in prior work [35,36,48], whose CNR is correlated with both psychosis severity in PSZ (measured as PANSS Positive subscale score) and subclinical positive symptom severity in persons at clinical high risk for developing a psychotic disorder [35,36].

PET data were acquired using procedures described elsewhere [49; and see Supplementary Methods]. Outcome measures included both baseline binding potential (BP_{ND}) and the fractional change in BP_{ND} following amphetamine administration,

$\Delta BP_{ND} = \frac{\mathrm{BP_{ND}(post-amph.)}}{\mathrm{BP_{ND}(baseline)}} - 1$, within a hand-drawn DCa ROI.

2.4. Statistical Analysis

Effect sizes for group differences in continuous variables were calculated using Hedges' *g* or Cliff's delta *d* for normally and non-normally distributed samples (as determined via Lilliefors test), respectively. Effect sizes for categorical and dichotomous variables were calculated as Cramér's *V* and phi coefficients, respectively, with p-values calculated using Chi-squared tests with significance level $p<0.05$. Group differences in continuous demographic variables and clinical assessments were assessed via independent samples t-tests or Mann-Whitney U-tests, depending on data normality. Group differences in SOT WM capacity *k* [41] and proportion of correct responses, both between HC and all PSZ and between HC and medication-naïve and medication-free PSZ separately, were assessed using Mann-Whitney U-tests.

Group differences in ROI pair FC were assessed via independent samples t-tests or Mann-Whitney U-tests, depending on data normality. The primary hypothesis investigating group differences in DCa-GPe rs-FC and ts-FC was assessed for significance (two-tailed) at $\alpha=0.05$ with Dunn–Šidák correction for the two comparisons testing our circuit-specific hypothesis arising from the D2R-OE mouse model. Post-hoc tests of group connectivity differences between all other ROI pairs were assessed separately at $\alpha=0.05$ with false discovery rate (FDR) correction across all tests [50], as we had no *a priori* hypotheses regarding connectivity

amongst this set of regions. The differing choice of Dunn–Šidák and FDR for these two cases is due to the greater sensitivity of the former when only two tests are performed, while the latter has greater sensitivity for a larger number of tests. As a supplementary analysis, we assessed group differences in DCa-GPe ts-FC and rs-FC using a robust multivariable linear regression with a Huber weight function with age and sex at birth as covariates.

Associations between DCa-GPe ts-FC and SOT performance [measured as WM capacity *k*; 41], average SN-VTA NM-MRI signal, [^{11}C]-(+)-PHNO baseline BP_{ND}, and ΔBP_{ND} were assessed via robust multivariable linear regression with a Huber weight function with age, sex at birth, and diagnosis as covariates; associations with PANSS Positive and Negative symptom scores were assessed in PSZ using the same covariates above except diagnosis. Associations with SN-VTA NM-MRI signal, baseline BP_{ND}, and ΔBP_{ND} were FDR-corrected (α=0.05) as they constitute a single family of tests concerning dopamine tone and function. All betas are reported as standardized regression coefficients β^*.

Supplementary statistical analyses investigating effects of previous medication exposure in PSZ, smoking status as a covariate, and regression analyses performed in HC and PSZ separately are described in the **Supplementary Methods**.

3. Results

3.1. Demographics

Thirty-seven PSZ and 30 HC completed at least two runs of resting-state fMRI (N=67), with zero participants excluded for excess motion. Additionally, 29 PSZ and 29 HC completed at least two runs of task-based fMRI (N=58), after excluding three PSZ and one HC due to excess motion. Summarized demographic information is shown in **Table 1**.

The median [IQR] SOT WM capacities (*k)* for HC and PSZ were 5.92 [1.61] and 4.73 [3.42], respectively (*P*=0.127; **Figure S4A**). The median [IQR] proportions of correct responses in HC and PSZ were 0.94 [0.08] and 0.88 [0.23], respectively (*P*=0.139; **Figure S4B**). In comparison

to medication-free PSZ, medication-naïve PSZ displayed greater task performance (median [IQR] proportion correct of 0.83 [0.21] in medication-free and 0.97 [0.15] in medication-naïve, *P*=0.018) and SOT *k* (median [IQR] of 3.64 [4.60] in medication-free and 5.94 [2.90] in medication-naïve, *P*=0.031). SOT *k* and proportion of correct responses were greater in HC than medication-free PSZ (*P*=0.007 and *P*=0.003, respectively, **Figure S4C, D**), but not medication-naïve PSZ (*P*=0.902 and *P*=0.664, respectively).

3.2. Resting-state and Task-state Functional Connectivity

No significant group difference in DCa-GPe rs-FC was observed (median [IQR] of 0.05 [0.16] in HC and 0.08 [0.12] in PSZ, *P*=0.233; **Figure 2C**). In contrast, PSZ displayed significantly elevated DCa-GPe ts-FC relative to HC (mean [SD] of 0.05 [0.09] in HC and 0.11 [0.10] in PSZ, *P*=0.0252**; Figure 2D**). This pattern of significance between rs-FC and ts-FC remained when group differences were assessed via robust regression controlling for age and sex at birth (**Tables S1, 2**). The group difference in DCa-GPe ts-FC remained significant when additionally controlling for smoking status (**Table S3**), while no group difference in rs-FC was observed (**Table S4**).

No significant differences between medication-naïve and medication-free PSZ were observed in DCa-GPe ts-FC (mean [SD] of 0.12 [0.11] in medication-free and 0.10 [0.09] in medication-naïve, *P*=0.638) or rs-FC (median [IQR] of 0.07 [0.10] in medication-free and 0.08 [0.15] in medication-naïve, *P*=0.891). Additionally, no significant differences in DCa-GPe ts-FC or rs-FC were observed between HC and medication-naïve or medication-free PSZ when assessed separately (**Figure S5**), though both had comparable effect sizes to the primary group difference between HC and all PSZ, suggesting inadequate power for subgroup analyses.

Within other direct connections in the BGTC circuit, HC displayed greater MD-DCa rs-FC than PSZ (mean [SD] of 0.27 [0.12] in HC and 0.17 [0.15] in PSZ, *P*=0.005**; Figure S6H**). No significant differences in ts-FC were observed following FDR correction (**Figure S7**), although MD-DLPFC ts-FC was significantly elevated in PSZ before correction. Medication-naïve PSZ

displayed lower DCa-SN rs-FC than HC (**Figure S8B**), and medication-free PSZ displayed lower MD-DCa rs-FC than HC (**Figure S8H**). No additional ts-FC differences were observed between HC and medication-naïve or medication-free PSZ separately after FDR correction (**Figure S9**).

3.3. Neuromelanin-Sensitive MRI

The average NM-MRI contrast-ratio map across participants is shown in **Figure 3A**. In *a priori* psychosis-associated voxels [35,36], SN/VTA NM-MRI CNR was positively associated with DCa-GPe ts-FC (N=42; β* [SE]=0.40 [0.17], *P*=0.023**; Figure 3B**, **Table S5**) when controlling for age, sex at birth, and diagnosis, and survives FDR correction at α=0.05. This association remains significant when controlling for smoking status (**Table S6**). When investigating groups separately, the association remains significant in PSZ (N=22; β* [SE]=0.55 [0.22], *P*=0.019**; Table S7**) regardless of controlling for smoking status (**Table S8**). Finally, no significant effects of medication exposure or its interaction with DCa-GPe ts-FC were observed in PSZ (**Table S9**).

3.4. [^{11}C]-(+)-PHNO Positron Emission Tomography

In the exploratory [^{11}C]-(+)-PHNO PET sample, elevated DCa-GPe ts-FC was significantly negatively associated with DCa baseline D2R availability, measured as [^{11}C]-(+)-PHNO BP_{ND} (N=11; β* [SE]=-0.45 [0.17], *P*=0.039; **Figure S10A, Table S10**). Additionally, greater DCa-GPe ts-FC was associated with more negative DCa ΔBP_{ND} (N=11; β* [SE]=-0.82 [0.27], *P*=0.021; **Figure S10B**, **Table S10**), where a more negative ΔBP_{ND} indicates greater fractional decrease in BP_{ND} following amphetamine administration. Both results survive FDR correction at α=0.05. After controlling for smoking status, there are no significant associations between DCa-GPe ts-FC and baseline BP_{ND} or ΔBP_{ND} (**Table S11**).

3.5. Associations between Task-state Functional Connectivity and Symptomatology

Elevated DCa-GPe ts-FC was associated with lower SOT *k* across all participants (N = 58; β* [SE]=-0.31 [0.13], *P*=0.020**; Figure 4A**, **Table S12**). This association remains significant

when controlling for smoking status (**Table S13**) and within PSZ alone (N=29; β* [SE]=-0.36 [0.15], *P*=0.029; **Table S14**; see **Table S15** for inclusion of smoking status as a covariate), but not in HC. Finally, there was no significant interaction of medication exposure and DCa-GPe ts-FC in predicting SOT *k* (**Table S16**).

In PSZ, no significant associations were observed between DCa-GPe ts-FC and PANSS Positive symptom score (N=27; β* [SE]=-0.39 [0.21], *P*=0.068**; Figure 4B, Table S17**) or PANSS Negative symptom score (N=27; β* [SE]=-0.20 [0.23], *P*=0.389**; Figure 4C, Table S17**).

4. Discussion

The results presented here support our hypothesis of specifically altered dorsal caudate-globus pallidus externus (DCa-GPe) connectivity in unmedicated persons with schizophrenia, consistent with reorganization of this circuitry observed in the D2R-OE mouse model [9,12] of striatal dopamine dysfunction in schizophrenia. Our findings also provide multiple lines of evidence that this alteration is associated with striatal dopamine dysfunction and WM deficits, consistent with dopaminergic and behavioral deficits observable in D2R-OE mice.

We demonstrated DCa-GPe hyperconnectivity in unmedicated PSZ that is observable during performance of a WM task, but not in the resting state, consistent with the observation that striatal MSNs projecting to GPe are relatively quiet at rest due to a low intrinsic resting membrane potential [19,20], which may prevent detection of altered fMRI connectivity unless receiving stimulation from cortical and thalamic inputs during cognitive processing. The results of secondary analyses are also consistent with our hypotheses, with significant correlations between DCa-GPe ts-FC and WM as well as all dopaminergic outcome measures collected in our sample (although PET results should be considered preliminary given the small sample size). DCa-GPe ts-FC was specifically elevated, rather than part of a broader alteration of ts-FC throughout the BGTC network (see **Figure S7**).

Consistent with evidence of dopaminergic control of bridging collateral density in D2R-OE mice, our findings suggest a role for subcortical dopamine dysfunction in altered striato-pallidal

functional connectivity in PSZ. NM-MRI signal in the SN and VTA is a proxy measure of long-term dopamine turnover [unless neuronal cell death has occurred, e.g., in Parkinson's disease; 35,36] that was associated with psychotic symptom severity in prior work [51]. One potential source of elevated nigral NM signal is upregulated dopamine turnover in nigral cell bodies, which is suggested by PET studies of PSZ using [^{18}F]DOPA [1,2,4] and may result in elevated presynaptic availability and release in striatum [52], a well-established finding in PSZ linked to psychosis severity [5,7,8,17]. Although observed in a small exploratory sample of PSZ and HC, our finding that individuals who show stronger dopamine release following amphetamine challenge have more greatly elevated DCa-GPe connectivity provides preliminary support for this interpretation. Similarly, decreased baseline D2R availability was also associated with DCa-GPe hyperconnectivity in our PET sample, which could be due to increased baseline availability of dopamine in the DCa that competes with radiotracer binding, resulting in lower BP_{ND} in these participants. However, we cannot rule out the possibility that lower D2R density in DCa also contributes to lower BP_{ND}.

Finally, we found that elevated DCa-GPe ts-FC is associated with poorer WM task performance; this association remains significant in PSZ alone and is analogous to performance deficits in a T-maze WM task observed in D2R-OE mice [9]. Given that these deficits in D2R-OE mice remained when upregulation of DCa-GPe bridging collaterals was normalized via D2R antagonist antipsychotic administration, this finding suggests DCa-GPe hyperconnectivity could be a state-dependent predictor of the neurodevelopmental impact of persistent dopamine dysfunction in PSZ prior to becoming medicated. That is, unmedicated PSZ with more severe subcortical dopamine dysfunction may develop greater bridging collateral density between DCa and GPe, driving further BGTC circuit reorganization that disrupts the maintenance of internal representations of task stimuli in prefrontal cortical regions, e.g., via effects on D1R function in DLPFC, which is thought to be disrupted in PSZ [53], critical for WM, and altered in D2R-OE mice [9,54]. A potential mechanism for this resulting cortical dysfunction is the persistent

functional abnormalities that exist in dopamine neurons of D2R-OE mice, particularly decreased phasic activity and neuronal recruitment under WM task demands [55]. These abnormalities may not be normalized via antipsychotic medication administered after their development, resulting in persistent WM deficits.

While these results provide support for our hypothesis of dopamine-driven alterations to DCa-GPe connectivity in PSZ, several caveats and limitations must be acknowledged. First, alternative interpretations of elevated DCa-GPe ts-FC in PSZ are plausible given that rs-fMRI and task-based fMRI cannot discern patterns of DCa-GPe structural connectivity, which should be further investigated using diffusion weighted imaging. Next, group differences in WM performance were only observed between HC and medication-free PSZ, not with medication-naïve PSZ. Medication-naïve PSZ performed slightly better on the SOT than HC, which suggests this sample represents a high-functioning, psychiatrically stable outpatient population. While this limits claims that can be made about the relevance of previous dopamine antagonist medication exposure to basal ganglia connectivity alterations explored in this study, we still observe comparable effect sizes in group differences in DCa-GPe ts-FC between both PSZ groups separately and HC (**Figure S5B**) to the effect size observed between HC and all PSZ. Additionally, no significant medication exposure effects were observed in regressions predicting SOT *k* or SN-VTA NM CNR from DCa-GPe ts-FC, which remains a significant predictor of both outcomes when tested in PSZ alone.

Next, limitations in sample size in both the RS fMRI and PET samples may limit the generalizability of the presented results. While larger than the task-based fMRI sample, the RS fMRI sample may have lacked statistical power to detect significant group differences in DCa-GPe connectivity at smaller effect sizes, although the observed difference trended in the expected direction. However, the RS fMRI sample did possess sufficient power to detect a larger effect in MD-DCa hypoconnectivity in PSZ (**Figure S6**), a finding consistent with previous work [56-58]. The PET sample should be considered preliminary, as it was a small sample with

markedly younger PSZ than other samples in this study. Further, associations between PET metrics and DCa-GPe ts-FC did not survive when controlling for smoking status. Thus, we cannot claim associations between DCa baseline and ΔBP_{ND} and DCa-GPe ts-FC will generalize to larger, more variable samples of PSZ. Finally, no significant associations were observed between DCa-GPe ts-FC and PANSS Positive score. While we expected DCa-GPe connectivity may be an overall marker of disease severity, the lack of significant association may arise from statistical power limitations. Alternatively, DCa-GPe connectivity may more closely index the severity of a phenotype that leads to WM deficits in PSZ, rather than psychotic symptoms. This proposition would ideally be studied in a larger, transdiagnostic sample with WM ts-FC.

In summary, this study provides *in vivo* translational evidence of a neural abnormality between the DCa and GPe in unmedicated PSZ, consistent with findings from the D2R-OE transgenic mouse model. This abnormality was observed as elevated FC during WM task engagement and was associated with poor WM task performance and disrupted subcortical dopaminergic function measured by two imaging modalities. Future work should aim to demonstrate altered DCa-GPe structural connectivity, as well as examine the role of D2R antagonist antipsychotic medication in the normalization of the phenotype. Nevertheless, these results build on a rich literature implicating subcortical dopaminergic dysfunction in the pathophysiology of schizophrenia to suggest a neurodevelopmental mechanism of WM deficits in PSZ, a crucial step towards the development of novel therapeutic targets and treatments.

5. Data and Code Availability

All data and analysis code used in the preparation of this manuscript can be made available upon request to the corresponding author through a formal data sharing agreement.

6. Author Contributions

Conceptualization: J.X.V.S., A.A-D., C.K., and G.H.; **Data Curation:** P.N.T., J.C.W., Y.P., Z.J.Z., E.B.S-F., K.B., R.B.G., G.P., N.K.H., N.O., D.T.P., S.K.A., J.J.W., G.H., C.C., M.S., and J.X.V.S.; **Formal Analysis:** P.N.T., J.C.W., Y.P., D.T.P., Z.J.Z., M.S., C.C., and J.X.V.S.; **Funding Acquisition:** P.N.T., J.C.W., A.A-D., M.S., G.H., J.J.W., and J.X.V.S.; **Investigation:** P.N.T., J.C.W., Z.J.Z., R.B.G., E.B.S-F., K.B., G.P., D.T.P., N.O., N.K.H., S.K.A., J.J.W., M.S., A.A-D., G.H., C.C., and J.X.V.S.; **Methodology:** P.N.T., J.C.W., M.S., C.C., and J.X.V.S.; **Project Administration:** N.K.H., R.B.G., K.B., E.B.S-F., and J.X.V.S.; **Resources:** R.B.G., M.S., C.C., G.H., A.A-D., and J.X.V.S.; **Software:** P.N.T., J.C.W., S.K.A., Y.P., M.S., C.C., and J.X.V.S.; **Supervision:** R.B.G., N.K.H., G.P., J.J.W., M.S., G.H., C.C., A.A-D., and J.X.V.S.; **Validation:** P.N.T., J.C.W., Z.J.Z., Y.P., D.T.P., M.S., C.C., and J.X.V.S.; **Visualization:** P.N.T.; **Writing – Original Draft:** P.N.T., J.C.W., M.S., and J.X.V.S.; **Writing – Review & Editing:** P.N.T., J.C.W., G.P., G.H., A.A-D., C.K., M.S., C.C., and J.X.V.S.

7. Acknowledgements

Research reported in this publication was supported by the National Institute of Mental Health of the National Institutes of Health (NIH) under award numbers K01MH107763 to J.X.V.S., K23MH101637 to G.H., R01MH109635 to A.A-D., R01MH124858 to C.K., F30MH122136 to J.C.W, and K23MH115291 to J.J.W. P.N.T. was supported by the Stony Brook University Scholars in Biomedical Sciences Program (NIH Award No. T32GM148331; PI: Dr. Styliani-Anna [Stella] E. Tsirka). J.C.W. was also supported by a Research Supplement to Promote Diversity in Health-Related Research (3R01MH120293-04S1) and by the Stony Brook University Medical Scientist Training Program (Award Nos. T32GM008444 and T32GM158461; Principal Investigator: Dr. Michael A. Frohman). The Stony Brook high-performance SeaWulf computing system was supported by National Science Foundation (NSF) Award Nos. 1531492 (PI: Dr. Robert Harrison; co-PI: Dr. Yuefan Deng) and 2215987 (PI: Dr. Robert Harrison; co-PIs: Dr. Yuefan Deng, Dr. Eva Siegmann, and David Cyrille), and matching funds from the Empire

State Development's Division of Science, Technology and Innovation (NYSTAR) program contract C210148. The Stony Brook University Social, Cognitive, and Affective Neuroscience (SCAN) Center was supported by NSF Award No. 0722874 (PI: Dr. Turhan Canli). This content is solely the responsibility of the authors and does not necessarily represent the official views of the NIH, NSF, or NYSTAR.

The authors would like to thank Jaeyop Jeong, Sam R. Luceno, and Srineil Nizamabad for their contributions to fMRI preprocessing, Elizabeth Chan for assistance with data visualization, and Tram N.B. Nguyen and Dr. Benjamin A. Ely for helpful discussions. We would also like to acknowledge the substantial computing resources and technical assistance provided by Stony Brook Medicine Research Computing, with substantial support from Allen Zawada and James Xikis, as well as Stony Brook Research Computing and Cyberinfrastructure and the Institute for Advanced Computational Science at Stony Brook University for access to the high-performance SeaWulf computing system, with notable support from Fırat Coşkun, Daniel Wood, and David Carlson.

8. Disclosures

Drs. Cassidy and Horga are inventors on patents for the analysis of NM-MRI, licensed to Terran Biosciences, Inc., but have received no royalties. Drs. Cassidy and Horga have an investigator-initiated sponsored research agreement and a licensing agreement with Terran Biosciences, Inc. Dr. Slifstein reports having served as a paid consultant for Neurocrine Biosciences, Inc. and for Yale University. Dr. Abi-Dargham received consulting fees from Neurocrine Biosciences, Inc., from Abbvie, Inc., and from MapLight Therapeutics, Inc. Dr. Abi-Dargham holds stock options in Herophilus, Inc. and in Terran Biosciences, Inc. Dr. Abi-Dargham is a Deputy Editor for the journal *Biological Psychiatry*. All other authors report no competing interests.

References

1 Meyer-Lindenberg A, Miletich RS, Kohn PD, Esposito G, Carson RE, Quarantelli M, et al. Reduced prefrontal activity predicts exaggerated striatal dopaminergic function in schizophrenia. Nature Neuroscience. 2002;5(3):267-71.

2 McGowan S, Lawrence AD, Sales T, Quested D, Grasby P. Presynaptic Dopaminergic Dysfunction in Schizophrenia. Archives of General Psychiatry. 2004;61(2).

3 Egerton A, Chaddock CA, Winton-Brown TT, Bloomfield MAP, Bhattacharyya S, Allen P, et al. Presynaptic Striatal Dopamine Dysfunction in People at Ultra-high Risk for Psychosis: Findings in a Second Cohort. Biological Psychiatry. 2013;74(2):106-12.

4 Howes OD, Bose SK, Turkheimer F, Valli I, Egerton A, Valmaggia LR, et al. Dopamine Synthesis Capacity Before Onset of Psychosis: A Prospective [18F]-DOPA PET Imaging Study. American Journal of Psychiatry. 2011;168(12):1311-17.

5 Abi-Dargham A, Gil R, Krystal J, Baldwin RM, Seibyl JP, Bowers M, et al. Increased striatal dopamine transmission in schizophrenia: confirmation in a second cohort. Am J Psychiatry. 1998;155(6):761-7.

6 Breier A, Su TP, Saunders R, Carson RE, Kolachana BS, de Bartolomeis A, et al. Schizophrenia is associated with elevated amphetamine-induced synaptic dopamine concentrations: Evidence from a novel positron emission tomography method. Proceedings of the National Academy of Sciences. 1997;94(6):2569-74.

7 Kegeles LS, Abi-Dargham A, Frankle WG, Gil R, Cooper TB, Slifstein M, et al. Increased Synaptic Dopamine Function in Associative Regions of the Striatum in Schizophrenia. Archives of General Psychiatry. 2010;67(3).

8 Abi-Dargham A, Rodenhiser J, Printz D, Zea-Ponce Y, Gil R, Kegeles LS, et al. Increased baseline occupancy of D2 receptors by dopamine in schizophrenia. Proc Natl Acad Sci U S A. 2000;97(14):8104-9.

9 Kellendonk C, Simpson EH, Polan HJ, Malleret G, Vronskaya S, Winiger V, et al. Transient and Selective Overexpression of Dopamine D2 Receptors in the Striatum Causes Persistent Abnormalities in Prefrontal Cortex Functioning. Neuron. 2006;49(4):603-15.

10 Lee J, Park S. Working Memory Impairments in Schizophrenia: A Meta-Analysis. Journal of Abnormal Psychology. 2005;114(4):599-611.

11 Park S. Schizophrenics Show Spatial Working Memory Deficits. Archives of General Psychiatry. 1992;49(12).

12 Cazorla M, de Carvalho FD, Chohan MO, Shegda M, Chuhma N, Rayport S, et al. Dopamine D2 receptors regulate the anatomical and functional balance of basal ganglia circuitry. Neuron. 2014;81(1):153-64.

13 Alexander GE, Crutcher MD, DeLong MR. Chapter 6 Basal ganglia-thalamocortical circuits: Parallel substrates for motor, oculomotor, “prefrontal” and “limbic” functions. The Prefrontal Its Structure, Function and Cortex Pathology. 1991. p. 119-46.

14 Leisman G, Braun-Benjamin O, Melillo R. Cognitive-motor interactions of the basal ganglia in development. Front Syst Neurosci. 2014;8:16.

15 Lévesque M, Parent A. The striatofugal fiber system in primates: A reevaluation of its organization based on single-axon tracing studies. Proceedings of the National Academy of Sciences. 2005;102(33):11888-93.

16 Labouesse MA, Torres-Herraez A, Chohan MO, Villarin JM, Greenwald J, Sun X, et al. A non-canonical striatopallidal Go pathway that supports motor control. Nature Communications. 2023;14(1).

17 Howes OD, Kambeitz J, Kim E, Stahl D, Slifstein M, Abi-Dargham A, et al. The Nature of Dopamine Dysfunction in Schizophrenia and What This Means for Treatment. Archives of General Psychiatry. 2012;69(8).

18 Jueptner M, Weiller C. Review: Does Measurement of Regional Cerebral Blood Flow Reflect Synaptic Activity?—Implications for PET and fMRI. NeuroImage. 1995;2(2):148-56.

19 Kreitzer AC. Physiology and Pharmacology of Striatal Neurons. Annual Review of Neuroscience. 2009;32(1):127-47.

20 Wilson CJ, Groves PM. Spontaneous firing patterns of identified spiny neurons in the rat neostriatum. Brain research. 1981;220(1):67-80.

21 Masharipov R, Knyazeva I, Korotkov A, Cherednichenko D, Kireev M. Comparison of whole-brain task-modulated functional connectivity methods for fMRI task connectomics. Communications Biology. 2024;7(1).

22 Huang S, De Brigard F, Cabeza R, Davis SW. Connectivity analyses for task-based fMRI. Physics of Life Reviews. 2024;49:139-56.

23 Cole MW, Ito T, Cocuzza C, Sanchez-Romero R. The Functional Relevance of Task-State Functional Connectivity. The Journal of Neuroscience. 2021;41(12):2684-702.

24 Zhao W, Makowski C, Hagler DJ, Garavan HP, Thompson WK, Greene DJ, et al. Task fMRI paradigms may capture more behaviorally relevant information than resting-state functional connectivity. Neuroimage. 2023;270:119946.

25 Finn ES, Shen X, Scheinost D, Rosenberg MD, Huang J, Chun MM, et al. Functional connectome fingerprinting: identifying individuals using patterns of brain connectivity. Nat Neurosci. 2015;18(11):1664-71.

26 Greene AS, Gao S, Scheinost D, Constable RT. Task-induced brain state manipulation improves prediction of individual traits. Nat Commun. 2018;9(1):2807.

27 Greene AS, Gao S, Noble S, Scheinost D, Constable RT. How Tasks Change Whole-Brain Functional Organization to Reveal Brain-Phenotype Relationships. Cell Rep. 2020;32(8):108066.

28 Rosenberg MD, Finn ES, Scheinost D, Papademetris X, Shen X, Constable RT, et al. A neuromarker of sustained attention from whole-brain functional connectivity. Nat Neurosci. 2016;19(1):165-71.

29 Medaglia JD, Lynall ME, Bassett DS. Cognitive network neuroscience. J Cogn Neurosci. 2015;27(8):1471-91.

30 Bolt T, Nomi JS, Rubinov M, Uddin LQ. Correspondence between evoked and intrinsic functional brain network configurations. Hum Brain Mapp. 2017;38(4):1992-2007.

31 Cohen JR. The behavioral and cognitive relevance of time-varying, dynamic changes in functional connectivity. Neuroimage. 2018;180(Pt B):515-25.

32 Van Snellenberg JX, Slifstein M, Read C, Weber J, Thompson JL, Wager TD, et al. Dynamic shifts in brain network activation during supracapacity working memory task performance. Human Brain Mapping. 2015;36(4):1245-64.

33 Smith SM, Miller KL, Salimi-Khorshidi G, Webster M, Beckmann CF, Nichols TE, et al. Network modelling methods for FMRI. Neuroimage. 2011;54(2):875-91.

34 Marrelec G, Krainik A, Duffau H, Pélégrini-Issac M, Lehéricy S, Doyon J, et al. Partial correlation for functional brain interactivity investigation in functional MRI. NeuroImage. 2006;32(1):228-37.

35 Cassidy CM, Zucca FA, Girgis RR, Baker SC, Weinstein JJ, Sharp ME, et al. Neuromelanin-sensitive MRI as a noninvasive proxy measure of dopamine function in the human brain. Proceedings of the National Academy of Sciences. 2019;116(11):5108-17.

36 Wengler K, Baker SC, Velikovskaya A, Fogelson A, Girgis RR, Reyes-Madrigal F, et al. Generalizability and Out-of-Sample Predictive Ability of Associations Between Neuromelanin-Sensitive Magnetic Resonance Imaging and Psychosis in Antipsychotic-Free Individuals. JAMA Psychiatry. 2024;81(2).

37 Rabiner EA, Laruelle M. Imaging the D3 receptor in humans in vivo using [11C](+)-PHNO positron emission tomography (PET). The International Journal of Neuropsychopharmacology. 2010;13(03).

38 Caravaggio F, Nakajima S, Borlido C, Remington G, Gerretsen P, Wilson A, et al. Estimating Endogenous Dopamine Levels at D2 and D3 Receptors in Humans using the Agonist Radiotracer [11C]-(+)-PHNO. Neuropsychopharmacology. 2014;39(12):2769-76.

39 Health NIo. in *NIH RePORTER* (National Institutes of Health, Bethesda, MD, 2015).

40 Williams JC, Tubiolo PN, Gil RB, Zheng ZJ, Silver-Frankel EB, Haubold NK, et al. Auditory and Visual Thalamocortical Connectivity Alterations in Unmedicated People With Schizophrenia: An Individualized Sensory Thalamic Localization and Resting-State Functional Connectivity Study. Biol Psychiatry Cogn Neurosci Neuroimaging. 2025.

41 Van Snellenberg JX, Conway ARA, Spicer J, Read C, Smith EE. Capacity estimates in working memory: Reliability and interrelationships among tasks. Cognitive, Affective, & Behavioral Neuroscience. 2014;14(1):106-16.

42 Van Snellenberg JX, Girgis RR, Horga G, van de Giessen E, Slifstein M, Ojeil N, et al. Mechanisms of Working Memory Impairment in Schizophrenia. Biological Psychiatry. 2016;80(8):617-26.

43 Gratton C, Laumann TO, Nielsen AN, Greene DJ, Gordon EM, Gilmore AW, et al. Functional Brain Networks Are Dominated by Stable Group and Individual Factors, Not Cognitive or Daily Variation. Neuron. 2018;98(2):439-52.e5.

44 Elliott ML, Knodt AR, Cooke M, Kim MJ, Melzer TR, Keenan R, et al. General functional connectivity: Shared features of resting-state and task fMRI drive reliable and heritable individual differences in functional brain networks. Neuroimage. 2019;189:516-32.

45 Glasser MF, Sotiropoulos SN, Wilson JA, Coalson TS, Fischl B, Andersson JL, et al. The minimal preprocessing pipelines for the Human Connectome Project. NeuroImage. 2013;80:105-24.

46 Williams JC, Tubiolo PN, Luceno JR, Van Snellenberg JX. Advancing motion denoising of multiband resting-state functional connectivity fMRI data. NeuroImage. 2022;249.

47 Fair DA, Schlaggar BL, Cohen AL, Miezin FM, Dosenbach NUF, Wenger KK, et al. A method for using blocked and event-related fMRI data to study “resting state” functional connectivity. NeuroImage. 2007;35(1):396-405.

48 Ahrens J, Ford SD, Schaefer B, Reese D, Khan AR, Tibbo P, et al. Convergence of Cannabis and Psychosis on the Dopamine System. JAMA Psychiatry. 2025;82(6).

49 van de Giessen E, Weinstein JJ, Cassidy CM, Haney M, Dong Z, Ghazzaoui R, et al. Deficits in striatal dopamine release in cannabis dependence. Mol Psychiatry. 2017;22(1):68-75.

50 Benjamini Y, Hochberg Y. Controlling the False Discovery Rate: A Practical and Powerful Approach to Multiple Testing. Journal of the Royal Statistical Society: Series B (Methodological). 2018;57(1):289-300.

51 van der Pluijm M, Wengler K, Reijers PN, Cassidy CM, Tjong Tjin Joe K, de Peuter OR, et al. Neuromelanin-Sensitive MRI as Candidate Marker for Treatment Resistance in First-Episode Schizophrenia. American Journal of Psychiatry. 2024;181(6):512-19.

52 Vano LJ, McCutcheon RA, Rutigliano G, Kaar SJ, Finelli V, Nordio G, et al. Mesostriatal Dopaminergic Circuit Dysfunction in Schizophrenia: A Multimodal Neuromelanin-Sensitive Magnetic Resonance Imaging and [18F]-DOPA Positron Emission Tomography Study. Biological Psychiatry. 2024;96(8):674-83.

53 Abi-Dargham A, Javitch JA, Slifstein M, Anticevic A, Calkins ME, Cho YT, et al. Dopamine D1R Receptor Stimulation as a Mechanistic Pro-cognitive Target for Schizophrenia. Schizophrenia Bulletin. 2022;48(1):199-210.

54 Cazorla M, Shegda M, Ramesh B, Harrison NL, Kellendonk C. Striatal D2 Receptors Regulate Dendritic Morphology of Medium Spiny Neurons via Kir2 Channels. The Journal of Neuroscience. 2012;32(7):2398-409.

55 Duvarci S, Simpson EH, Schneider G, Kandel ER, Roeper J, Sigurdsson T. Impaired recruitment of dopamine neurons during working memory in mice with striatal D2 receptor overexpression. Nature Communications. 2018;9(1).

56 Anticevic A, Yang G, Savic A, Murray JD, Cole MW, Repovs G, et al. Mediodorsal and Visual Thalamic Connectivity Differ in Schizophrenia and Bipolar Disorder With and Without Psychosis History. Schizophrenia Bulletin. 2014;40(6):1227-43.

57 Welsh RC, Chen AC, Taylor SF. Low-Frequency BOLD Fluctuations Demonstrate Altered Thalamocortical Connectivity in Schizophrenia. Schizophrenia Bulletin. 2008;36(4):713-22.

58 Smith Y, Raju D, Nanda B, Pare J-F, Galvan A, Wichmann T. The thalamostriatal systems: Anatomical and functional organization in normal and parkinsonian states. Brain Research Bulletin. 2009;78(2-3):60-68.

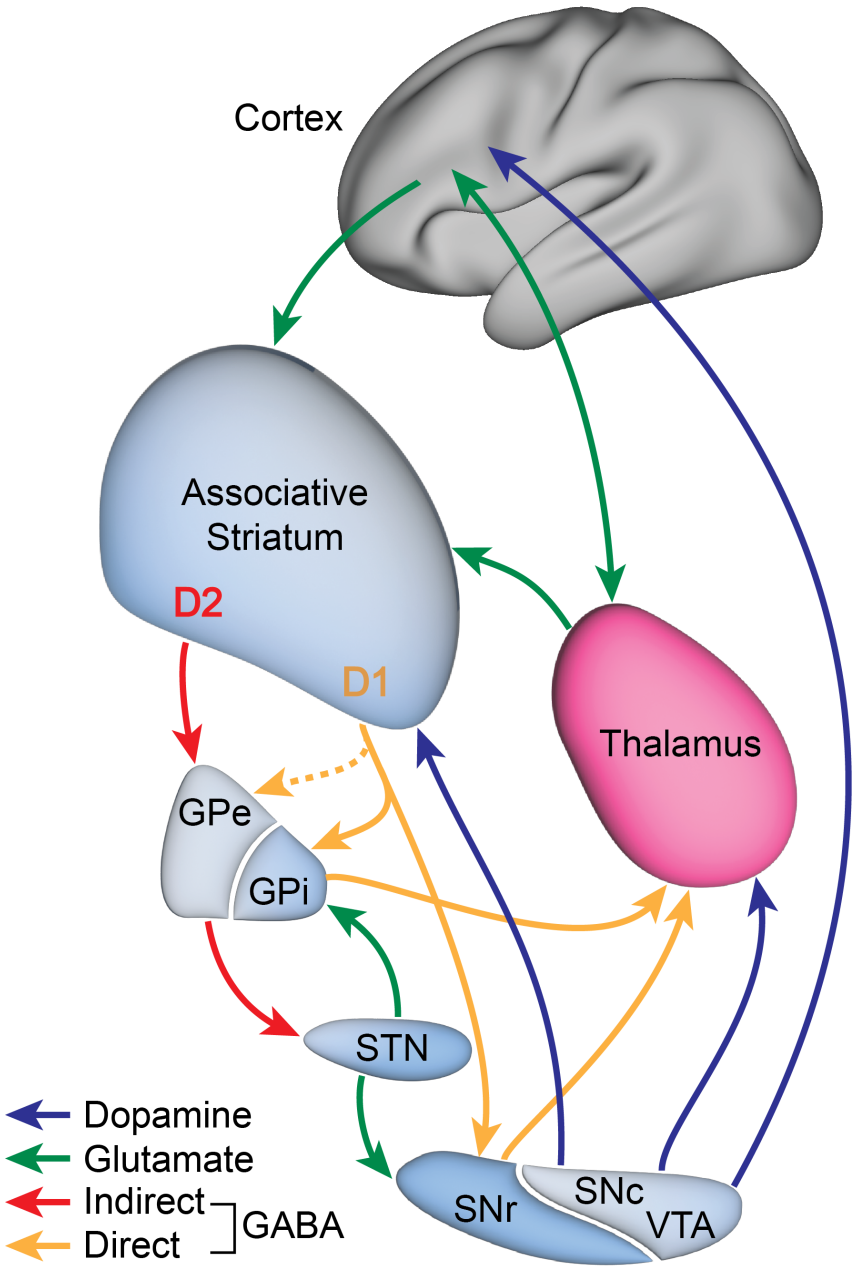

Figure 1. Schematic of basal ganglia-thalamo-cortical circuitry, highlighting glutamatergic (green arrows), GABAergic (red and orange arrows), and dopaminergic (blue arrows) connections between regions. Orange dashed line represents bridging collateral axonal projections from the associative striatum (primarily dorsal caudate) to the globus pallidus externus (GPe). GPi = globus pallidus internus; STN = subthalamic nucleus; SNr = substantia nigra pars reticulata; SNc = substantia nigra pars compacta; VTA = ventral tegmental area.

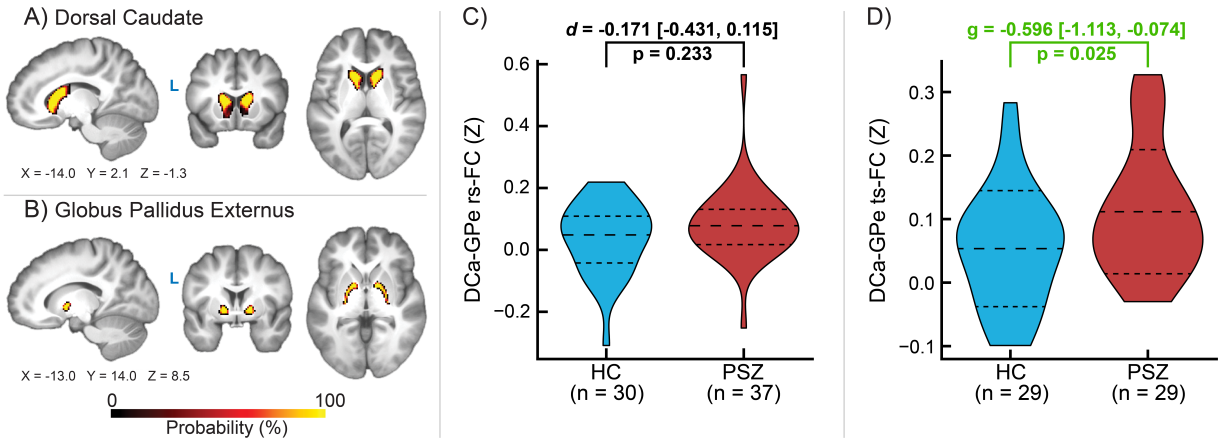

Figure 2. Probability density of **A)** dorsal caudate (DCa) and **B)** globus pallidus externus (GPe) regions of interest in the task-based fMRI sample (N = 58), as well as group differences between healthy controls (HC) and persons with schizophrenia (PSZ) in **C)** DCa-GPe resting-state functional connectivity (rs-FC) and **D)** DCa-GPe task-state functional connectivity (ts-FC). Long-dashed and short-dashed lines denote median and interquartile range in **Panel C** (due to non-normally distributed data) and means and standard deviations in **Panel D**. Both rs-FC and ts-FC were calculated while controlling for the average timeseries in dorsolateral prefrontal cortex, globus pallidus internus, substantia nigra, and mediodorsal nucleus. *g* = Hedges' *g* [95% Confidence Intervals]; *d* = Cliff's delta [95% Confidence Intervals].

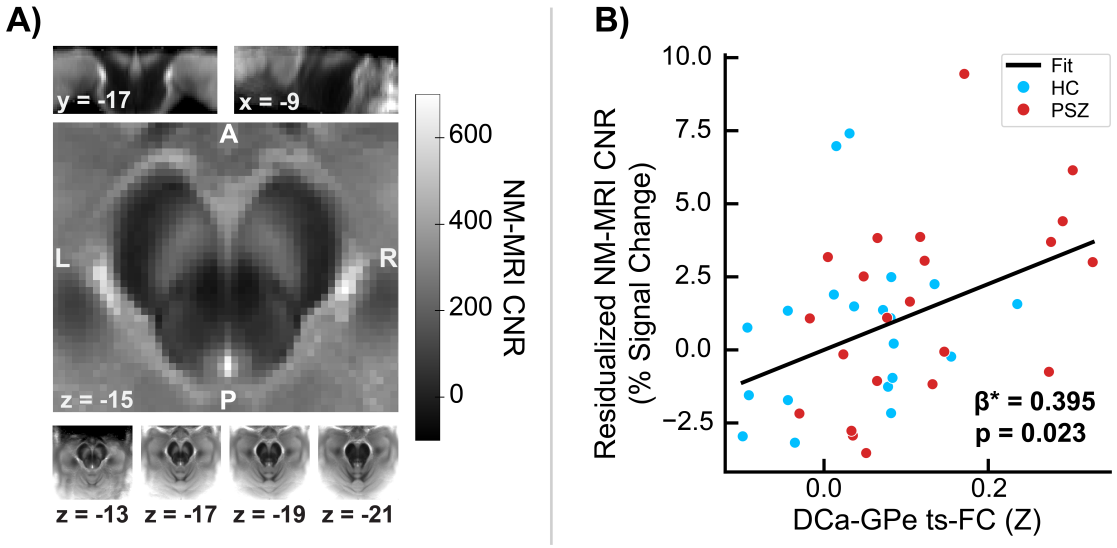

Figure 3. A) Average neuromelanin-sensitive MRI (NM-MRI) contrast-to-noise ratio (CNR) image across all participants (N = 42). **B)** Association between average substantia nigra – ventral tegmental area NM-MRI CNR and task-state functional connectivity (ts-FC) between dorsal caudate (DCa) and globus pallidus externus (GPe), controlling for age, sex at birth, and diagnosis (N = 42). Regression plot inlay shows standardized regression coefficient β*. Blue dots denote healthy controls; red dots denote persons with schizophrenia.

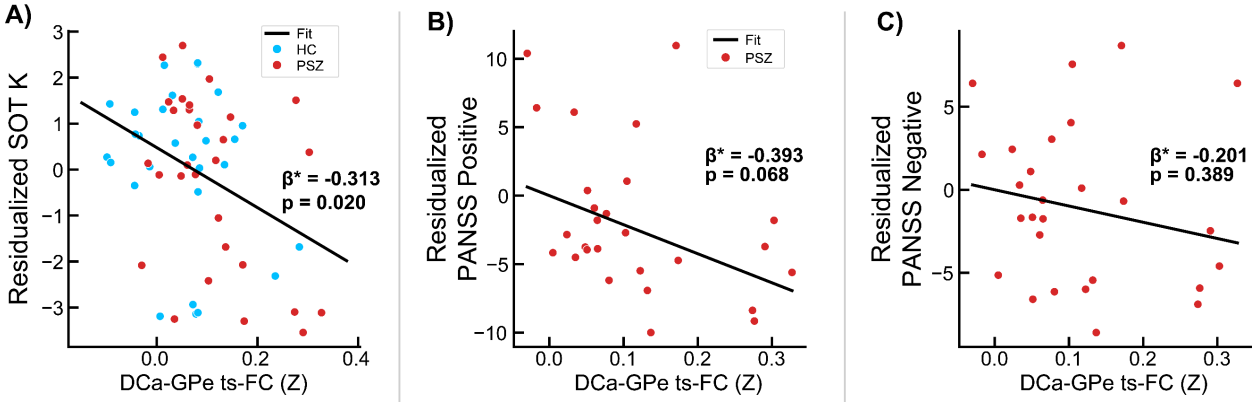

Figure 4. Associations between dorsal caudate-globus pallidus externus task-state functional connectivity (DCa-GPe ts-FC) and **A)** working memory capacity *k* calculated from self-ordered working memory task (SOT) performance, **B)** Positive and Negative Syndrome Scale (PANSS) Positive symptom score, and **C)** PANSS Negative symptom score. Associations between *k* and DCa-GPe ts-FC were calculated in all participants (N = 58), controlling for age, sex at birth, and diagnosis. PANSS symptom associations were calculated in persons with schizophrenia (PSZ; red) only (N = 27; PANSS data were unavailable for two PSZ), controlling for age and sex at birth. Plot inlays show standardized regression coefficient β*. Blue dots denote healthy controls (HC); red dots denote persons with schizophrenia (PSZ).

Table 1. Participant Demographics and Clinical Measures

Participant Characteristic	Task-Based (N = 58)				Resting State (N = 67)			
	PSZ (n = 29)	HC (n = 29)	Effect Size [95% CIs] [a]	P-value	PSZ (n = 37)	HC (n = 30)	Effect Size [95% CIs] [a]	P-value
Functional Magnetic Resonance Imaging Datasets								
Age, Years (SD)	33.4 (12.7)	32.4 (9.7)	-0.02 [-0.28, 0.32]	0.895	32.7 (12.7)	32.5 (9.7)	-0.06 [-0.21, 0.33]	0.659
Sex at Birth, Female (%)	9.0 (31.0%)	9.0 (31.0%)	0.0 [N/A]	1.00	11.0 (29.7%)	8.0 (26.7%)	0.03 [0, 0.29]	0.782
Ethnicity, Hispanic (%)	7.0 (24.1%)	8.0 (27.6%)	0.04 [0, 0.31]	0.764	9.0 (24.3%)	8.0 (26.7%)	0.03 [0, 0.27]	0.827
Race			0.16 [0, 0.41]	0.725			0.10 [0, 0.32]	0.992
African American (%)	14.0 (48.3%)	13.0 (44.8%)			18.0 (48.6%)	13.0 (43.3%)		
Asian (%)	3.0 (10.3%)	3.0 (10.3%)			3.0 (8.1%)	3.0 (10.0%)		
Caucasian (%)	6.0 (20.7%)	8.0 (27.6%)			9.0 (24.3%)	9.0 (30.0%)		
More than one (%)	4.0 (13.8%)	0.0 (0.0%)			3.0 (8.1%)	0.0 (0.0%)		
Other (%)	2.0 (6.9%)	5.0 (17.2%)			4.0 (10.8%)	5.0 (16.7%)		
Handedness[b]			0.19 [0, 0.47]	0.150			0.19 [0, 0.45]	0.111
Ambidextrous (%)	0.0 (0.0%)	0.0 (0.0%)			0.0 (0.0%)	0.0 (0.0%)		
Left (%)	0.0 (0.0%)	2.0 (6.9%)			0.0 (0.0%)	2.0 (6.7%)		
Right (%)	29.0 (100.0%)	27.0 (93.1%)			37.0 (100.0%)	28.0 (93.3%)		
Smoker[c,d] (%)	9.0 (31.0%)	3.0 (10.7%)	-0.26 [-0.53, 0]	0.052	11.0 (30.6%)	3.0 (10.3%)	-0.24 [-0.50,0]	**0.048**
Parental SES[e,f] (SD)	40.3 (13.9)	44.7 (11.2)	0.25 [-0.06, 0.52]	0.102	38.6 (14.3)	44.6 (11.0)	0.33 [-0.05, 0.57]	**0.020**
PANSS Total[g] (SD)	61.6 (18.3)	33.0 (4.8)	-0.92 [-0.98, -0.68]	**1.31×10^{-8}**	65.3 (18.0)	32.4 (2.9)	-2.35 [-3.01, -1.68] [†]	**7.34×10^{-12} [α]**
PANSS General[g] (SD)	31.4 (9.9)	17.0 (2.4)	-0.92 [-0.98, -0.72]	**5.73×10^{-9}**	33.2 (9.8)	16.7 (1.5)	-0.99 [-0.99, -0.96]	**3.25×10^{-11}**
PANSS Negative[g] (SD)	14.4 (4.8)	8.9 (2.7)	-0.72 [-0.87, -0.46]	**6.96×10^{-6}**	15.5 (5.3)	8.6 (2.3)	-0.81 [-0.91, -0.62]	**8.52×10^{-8}**
PANSS Positive[g] (SD)	15.9 (5.4)	7.2 (0.46)	-0.96 [-0.99, -0.78]	**5.87×10^{-10}**	16.6 (5.2)	7.1 (0.27)	-0.97 [-0.99, -0.82]	**4.48×10^{-11}**
CDRS[h] (SD)	3.1 (3.9)	0.17 (0.69)	-0.54 [-0.72, -0.28]	**5.76×10^{-4}**	3.7 (4.2)	0.17 (0.69)	-0.59 [-0.76, -0.35]	**1.81×10^{-4}**
AP Medication-Naïve[k] (%)	15 (51.7%)	—	—	—	18 (48.6%)	—	—	—
Median SOT % Correct (IQR)	88.0 (23.0)	94.0 (8.0)	0.23 [-0.09, 0.50]	0.139	—	—	—	—
Median SOT *k* (IQR)	4.73 (3.42)	5.92 (1.61)	0.23 [-0.08, 0.50]	0.127	—	—	—	—
	Positron Emission Tomography Dataset				***Neuromelanin-Sensitive MRI Dataset***			
	PSZ (n = 7)	HC (n = 4)	Effect Size [95% CIs] [a]	P-value	PSZ (n = 22)	HC (n = 20)	Effect Size [95% CIs] [a]	P-value
Age, Years (SD)	23.1 (6.3)	31.5 (11.9)	0.89 [-0.33, 2.06][†]	0.263[α]	35.1 (13.9)	29.4 (8.5)	-0.18 [-0.50, 0.19]	0.325
Sex at Birth, Female (%)	4 (57.1%)	1 (25.0%)	0.31 [0,0.95]	0.303	8 (36.4%)	7 (35.0%)	0.01 [0,0.27]	0.927
Ethnicity, Hispanic (%)	0 (0.0%)	1 (25.0%)	0.42 [0, 1.05]	0.165	4 (18.2%)	7 (35.0%)	0.19 [0, 0.52]	0.216
Race			0.52 [0, 1.11	0.402			0.28 [0, 0.59]	0.395
African American (%)	3 (42.9%)	2 (50.0%)			12 (54.5%)	8 (40.0%)		
Asian (%)	2 (28.6%)	0 (0.0%)			2 (9.1%)	2 (10.0%)		
Caucasian (%)	2 (28.6%)	1 (25.0%)			4 (18.2%)	6 (30.0%)		
More than one (%)	0 (0.0%)	0 (0.0%)			3 (13.6%)	0 (0.0%)		
Other (%)	0 (0.0%)	1 (25.0%)			1 (4.6%)	4 (20.0%)		
Handedness[b]			0.42 [0, 1.05]	0.165			0.23 [0, 0.56]	0.129
Ambidextrous (%)	0 (0.0%)	0 (0.0%)			0 (0.0%)	0 (0.0%)		
Left (%)	0 (0.0%)	1 (25.0%)			0 (0.0%)	2 (10.0%)		

Right (%)	7 (100.0%)	3 (75.0%)			22 (100.0%)	18 (90.0%)		
Smoker[c] (%)	2 (28.6%)	0 (0.0%)	-0.36 [-0.99, 0]	0.237	6 (27.3%)	3 (15.0%)	-0.15 [-0.48, 0]	0.332
Parental SES[e,f] (SD)	46.8 (15.8)	34.6 (5.9)	-0.43 [-0.85, 0.32]	0.315	42.1 (13.4)	45.7 (10.2)	0.29 [-0.31, 0.89] †	0.336 [α]
PANSS Total[g] (SD)	78.6 (21.5)	33.5 (4.5)	-2.32 [-3.82, -0.74] †	**0.001[α]**	64.4 (19.3)	32.8 (3.1)	-2.16 [-2.94, -1.37] †	**2.57 x10^{-7} [α]**
PANSS General (SD)	39.7 (14.3)	17.8 (2.9)	-1.70 [-3.03, -0.30] †	**0.006[α]**	32.8 (10.6)	16.6 (1.5)	-0.99 [-1.00, -0.92]	**6.74 x10^{-8}**
PANSS Negative (SD)	19.1 (3.8)	8.8 (1.7)	-2.91 [-4.61, -1.15] †	**1.72 x10^{-4} [α]**	14.8 (5.1)	9.1 (2.6)	-0.74 [-0.88, -0.45]	**7.64 x10^{-5}**
PANSS Positive (SD)	19.7 (5.6)	7.0 (0)	-2.52 [-4.09, -0.88] †	**0.001[α]**	16.9 (5.7)	7.1 (0.3)	-2.29 [-3.09, -1.48] †	**1.40 x10^{-7} [α]**
CDRS[h] (SD)	6.4 (5.3)	0.8 (1.5)	-0.71 [-0.94, -0.03]	0.079	3.4 (4.2)	0.2 (0.8)	-0.55 [-0.75, -0.27]	**0.001**
AP Medication-Naïve[k] (%)	7 (100%)	—	—	—	11 (50.0%)	—	—	—

[a]Effect sizes for continuous variables were calculated with Hedges's g or Cliff's delta *d,* dependent on data normality (determined via Lilliefors test with a null hypothesis that data originates from a normal distribution at significance level p<0.05). Effect sizes for dichotomous and categorical variables were calculated with phi coefficients and Cramér's V, respectively.
[b]Handedness was reported using the Edinburgh Handedness Inventory.
[c]Smoking status defined as current daily nicotine use.
[d]Smoking status was unavailable for 2 participants (1 PSZ and 1 HC) from the resting-state sample and 1 HC from the task-based sample.
[e]Mean Parental SES was reported using the Hollingshead Four Factor Index Scale of Socioeconomic Status scale.
[f]Parental SES data were unavailable for 7 participants (5 PSZ and 2 HC) from the resting-state sample, 4 participants (2 PSZ and 2 HC) from the task-based sample, and 2 HC from the neuromelanin-sensitive MRI sample.
[g]PANSS data were unavailable for 8 participants (4 PSZ and 4 HC) from the resting-state sample, 6 participants (2 PSZ and 4 HC) from the task-based sample, and 3 participants (1 PSZ and 2 HC) from the neuromelanin-sensitive MRI sample.
[h]CDRS data were unavailable for 22 participants (10 PSZ and 12 HC) in the resting-state sample, 16 participants (5 PSZ and 11 HC) in the task-based sample, and 6 participants (2 PSZ and 4 HC) in the neuromelanin-sensitive MRI sample.
[k]All PSZ in this study were antipsychotic-free, defined as no exposure to oral antipsychotic medication for at least 3 weeks, and no exposure to intramuscular antipsychotic medications for at least 6 months, prior to study participation. PSZ were considered to be medication-naïve if they had fewer than 2 weeks of cumulative lifetime exposure to antipsychotic medications, with no prior use of long-acting injectable antipsychotics.
[α] Indicates use of independent samples t-test, rather than Mann-Whitney U-test, to obtain p-value.
† Indicates effect sizes for continuous variable calculated as Hedges's g, rather than Cliff's delta *d.*
Bold p-values indicate significance at p<0.05 (uncorrected).

Abbreviations: PSZ: Persons with Schizophrenia; HC: Healthy Controls; SD: standard deviation; SES: socioeconomic status; PANSS: Positive and Negative Syndrome Scale; CDRS: Calgary Depression Scale for Schizophrenia; AP: Antipsychotic; SOT: Self-ordered Working Memory Task; *k*: Working Memory Capacity; IQR: Interquartile Range; CIs: Confidence Intervals.